Fractional Quantum Hall Effect with Unconventional Pairing in Monolayer Graphene

Anirban Sharma,[1] Songyang Pu,[1,2] Ajit C. Balram,[3,4] and J. K. Jain[1]
[1]Department of Physics, 104 Davey Lab, Pennsylvania State University, University Park, Pennsylvania 16802, USA
[2]School of Physics and Astronomy, University of Leeds, Leeds LS2 9JT, United Kingdom
[3]Institute of Mathematical Sciences, CIT Campus, Chennai, 600113, India
[4]Homi Bhabha National Institute, Training School Complex, Anushaktinagar, Mumbai, 400094, India

(Received 30 August 2022; accepted 24 February 2023; published 21 March 2023)

Motivated by the observation of even denominator fractional quantum Hall effect in the $n = 3$ Landau level of monolayer graphene [Kim *et al.*, Nat. Phys. **15**, 154 (2019)], we consider a Bardeen-Cooper-Schrieffer variational state for composite fermions and find that the composite-fermion Fermi sea in this Landau level is unstable to an f-wave pairing. Analogous calculation suggests the possibility of a p-wave pairing of composite fermions at half filling in the $n = 2$ graphene Landau level, whereas no pairing instability is found at half filling in the $n = 0$ and $n = 1$ graphene Landau levels. The relevance of these results to experiments is discussed.

DOI: 10.1103/PhysRevLett.130.126201

The $\nu = 5/2$ fractional quantum Hall effect (FQHE) at half-filled second Landau level (LL) in semiconductor quantum wells [1] has been modeled through a Moore-Read (MR) Pfaffian wave function, which represents a p-wave paired state of the spin-polarized composite fermions (CFs) [2,3], where the CF is a topological particle composed of an electron and an even number of quantized vortices [4,5]. This raises the question of whether CF pairs with other symmetry can also be realized.

Which FQHE state occurs depends on the Haldane pseudopotentials V_m [6] (V_m is the energy of two electrons in a state with relative angular momentum m), which, in turn, are determined by both the interaction and the LL in which the electrons reside. Graphene provides a platform for realizing many old as well as new FQHE states. Unexpectedly, an FQHE state has been observed at half-filling in the $n = 3$ LL of monolayer graphene [7]. Reference [7] considered many candidate FQHE states and concluded that while none matches the Coulomb ground state, the 221 parton state [8] defined below is the most promising because it can be stabilized when the V_1 and V_3 pseudopotentials are varied slightly away from their pure Coulomb values. A realization of this state would be of interest because it represents an f-wave pairing of CFs [9,10] and supports Ising type non-Abelian quasiparticles [11,12]. It is also the exact ground state [12,13] for the short range Trugman-Kivelson model interaction [14]. The 221 and the related 22111 states have been shown theoretically to be promising candidates also for $1/2$ FQHE in multilayer graphene [13] and $1/4$ FQHE [10] observed in wide quantum wells [15–17].

We investigate in this work the possibility of CF pairing in monolayer graphene directly from the Bardeen-Cooper-Schrieffer (BCS) perspective. Such an approach has previously been used in the contexts of p-wave CF pairing at $\nu = 5/2$ [18,19] and s- and p-wave CF pairing in bilayer systems [20]. We consider more general pairings to address even-denominator FQHE in graphene. We employ a BCS wave function of CFs in the torus (periodic) geometry, which is convenient for momentum space pairing [19]. This wave function has two variational parameters, analogous to the gap function and the Debye cutoff of the standard BCS theory. An advantage of this method is that it enables a study of the competition between different kinds of pairing instabilities. Specifically, we can choose the gap function as $\Delta_{\boldsymbol{k}}^{(l)} \sim e^{-il\theta}$, where θ is the angular coordinate of the wave vector $\boldsymbol{k}$, and the relative angular momentum l must be an odd integer for fully spin-polarized fermions. The choice $l = 1$ corresponds to p-wave pairing and $l = 3$ to f wave (in our convention of magnetic field B pointing in the $-z$ direction). Another advantage of this method is that it allows minimization of energy by adjusting parameters and thus may capture physics missed in studies that use a single, fixed wave function. Finally, the various paired states are explicitly seen to arise through an instability of the CF Fermi sea (CFFS), which is a special case of the CF-BCS wave function. Reference [19] demonstrated that this approach is capable of capturing the p-wave pairing instability at $\nu = 5/2$ in semiconductor systems.

We find that the CFFS is unstable to f-wave pairing at half filling in the $n = 3$ graphene LL. Notably, this instability is seen without any modification to the Coulomb interaction. No pairing instability occurs in the $n = 0$ or $n = 1$ graphene LL, but our work suggests the possibility of p-wave pairing in the $n = 2$ graphene LL.

Our starting point is the BCS wave function for CFs on a torus. We consider a torus defined by a parallelogram with sides L and $L\tau$, where the complex number $\tau = \tau_1 + i\tau_2$

specifies the modular parameter of the torus [21]. The allowed values of wave vectors are $\boldsymbol{k} = [n_1 + (\phi_1/2\pi)]\boldsymbol{b_1} + [n_2 + (\phi_2/2\pi)]\boldsymbol{b_2}$, with $\boldsymbol{b}_1 = [(2\pi/L), -(2\pi\tau_1/L\tau_2)]$, $\boldsymbol{b}_2 = [0, (2\pi/L\tau_2)]$, where ϕ_j represent twisted phase in quasiperiodic boundary conditions. We take $\phi_1 = \phi_2 = \pi$ in what follows, to ensure that $\boldsymbol{k} = 0$ is not an allowed value, and for each $\boldsymbol{k}$, $-\boldsymbol{k}$ is also allowed. We define $z_j = x_j + iy_j$, where $\boldsymbol{r}_j \equiv (x_j, y_j)$ are the coordinates of the jth electron.

The BCS wave function for fully spin-polarized electrons is written as $|\Psi_{\rm BCS}\rangle = \prod'_{\boldsymbol{k}}(u_{\boldsymbol{k}} + v_{\boldsymbol{k}} c^\dagger_{\boldsymbol{k}} c^\dagger_{-\boldsymbol{k}})|0\rangle$, where $|0\rangle$ is the null state; $c^\dagger_{\boldsymbol{k}}$ creates an electron at $\boldsymbol{k}$; each $\boldsymbol{k}$, $-\boldsymbol{k}$ is counted only once in the product; and $|v_{\boldsymbol{k}}|^2$ ($|u_{\boldsymbol{k}}|^2$) is the probability of this state to be occupied (empty). The real space form of the BCS wave function for a fixed number of electrons is given by [22]

$$\Psi_{\rm BCS}(\boldsymbol{r}_1, \ldots \boldsymbol{r}_N) = {\rm Pf}[g^{(l)}(\boldsymbol{r}_i - \boldsymbol{r}_j)], \tag{1}$$

where Pf refers to Pfaffian, and the antisymmetric matrix element $g^{(l)}(\boldsymbol{r}_i - \boldsymbol{r}_j)$ can be expanded as

$$g^{(l)}(\boldsymbol{r}_i - \boldsymbol{r}_j) = \sum_{\boldsymbol{k}} g^{(l)}_{\boldsymbol{k}} e^{i\boldsymbol{k}\cdot(\boldsymbol{r}_i - \boldsymbol{r}_j)} \tag{2}$$

with

$$g^{(l)}_{\boldsymbol{k}} \equiv v_{\boldsymbol{k}}/u_{\boldsymbol{k}} = [\epsilon_{\boldsymbol{k}} - \sqrt{\epsilon^2_{\boldsymbol{k}} + |\Delta^{(l)}_{\boldsymbol{k}}|^2}]/\Delta^{(l)*}_{\boldsymbol{k}} = -g^{(l)}_{-\boldsymbol{k}}. \tag{3}$$

Here $\epsilon_{\boldsymbol{k}} = \hbar^2(|\boldsymbol{k}|^2 - k_F^2)/2m_e$ (we determine the magnitude of k_F using the relation: $\pi|k_F|^2 = N|\boldsymbol{b}_1 \times \boldsymbol{b}_2|$), and the gap function for the l pairing channel has the form $\Delta^{(l)}_{\boldsymbol{k}} = \Delta|\boldsymbol{k}|e^{-il\theta}$. (This form corresponds to the real space pair wave function of the form $e^{il\theta}/|z_i - z_j|$ for large $|z_i - z_j|$.) The alternative choice $\Delta^{(l)}_{\boldsymbol{k}} = \Delta|\boldsymbol{k}|^l e^{-il\theta}$ is equivalent in the limit where only wave vectors near the Fermi surface are relevant to pairing, in which case $|\boldsymbol{k}|$ may be replaced by k_F; our explicit calculations shown in the Supplemental Material [23] demonstrate that the conclusions are not affected by this detail.

The BCS wave function for CFs at $\nu = 1/2$ can now be constructed in the standard manner by vortex attachment [4,5]. In the disk geometry, one would write $\Psi^{\rm CF-BCS} \sim P_{\rm LLL}{\rm Pf}[g^{(l)}(\boldsymbol{r}_i - \boldsymbol{r}_j)]\prod_{j<k}(z_j - z_k)^2$, where $P_{\rm LLL}$ refers to lowest-LL (LLL) projection. One would then attempt to implement the Jain Kamilla (JK) projection into the LLL [33,34] by writing the Jastrow factor as $\prod_{j<k}(z_j - z_k)^2 = \prod_i J_i$, where $J_i = \prod_{k\neq i}(z_i - z_k)$; incorporating it into the Pfaffian as $\Psi^{\rm CF-BCS} \sim P_{\rm LLL}{\rm Pf}[g^{(l)}(\boldsymbol{r}_i - \boldsymbol{r}_j)J_iJ_j]$ [35]; and then projecting each matrix element separately into the LLL. In the torus geometry, we write

$$\Psi^{\rm CF-BCS}_{\frac{1}{2}} = P_{\rm LLL}{\rm Pf}\left(\sum_{\boldsymbol{k}} g^{(l)}_{\boldsymbol{k}} e^{i\boldsymbol{k}\cdot(\boldsymbol{r}_i - \boldsymbol{r}_j)}\right)\Psi^{\rm L}_{1/2}, \tag{4}$$

where $\Psi^{\rm L}_{1/2}$ is the $\nu = 1/2$ Laughlin wave function [36] in the torus geometry [37–39], while also replacing the mass of electron m_e in Eq. (3) by the CF effective mass of m^*. An implementation of the standard JK projection [33,34] in the torus geometry yields unphysical wave functions that do not satisfy the stipulated periodic boundary conditions (PBC). However, a modified JK projection accomplishes the task [19,40,41]. The resulting LLL wave function has the form (see Ref. [19] and Supplemental Material [23] for details)

$$\Psi^{\rm CF-BCS}_{\frac{1}{2}} = e^{\sum_i \frac{z_i^2 - |z_i|^2}{4\ell^2}}\left\{\vartheta\begin{bmatrix}\frac{\phi_1}{4\pi} + \frac{N_\phi - 2}{4} \\ -\frac{\phi_2}{2\pi} + N - 1\end{bmatrix}\left(\frac{2Z}{L}\middle|2\tau\right)\right\}{\rm Pf}(M_{ij}), \tag{5}$$

$$M_{ij} = \sum_{\boldsymbol{k}} g_{\boldsymbol{k}} e^{-\frac{\ell^2}{2}k(k+2\bar{k})} e^{\frac{i}{2}(z_i - z_j)(k+\bar{k})}\left(\vartheta\begin{bmatrix}\frac{1}{2} \\ \frac{1}{2}\end{bmatrix}\left(\frac{z_i + ik\ell^2 - (z_j - ik\ell^2)}{L}\middle|\tau\right)\right)^2$$
$$\times\left\{\prod_{\substack{r \\ r\neq i,j}}\vartheta\begin{bmatrix}\frac{1}{2} \\ \frac{1}{2}\end{bmatrix}\left(\frac{z_i + i2k\ell^2 - z_r}{L}\middle|\tau\right)\prod_{\substack{m \\ m\neq i,j}}\vartheta\begin{bmatrix}\frac{1}{2} \\ \frac{1}{2}\end{bmatrix}\left(\frac{z_j - i2k\ell^2 - z_m}{L}\middle|\tau\right)\right\}. \tag{6}$$

Here $Z = \sum_{i=1}^N z_i$ is the center-of-mass (c.m.) coordinate, $k = k_x + ik_y$, $\ell = \sqrt{\hbar c/eB}$ is the magnetic length, N is the number of particles, and $N_\phi = 2N$ is the number of flux quanta through the torus. The Jacobi theta function with rational characteristics is defined as [42] $\vartheta\begin{bmatrix}a \\ b\end{bmatrix}(z|\tau) = \sum_{n=-\infty}^{\infty} e^{i\pi(n+a)^2\tau}e^{i2\pi(n+a)(z+b)}$. The above BCS wave function satisfies proper quasiperiodic boundary conditions on the torus. In terms of a dimensionless "gap parameter" $\tilde{\Delta} = |\Delta^{(l)}_{k_F}|/(\hbar^2|k_F|^2/2m^*)$, we have $g^{(l)}_{\boldsymbol{k}} = [|\boldsymbol{k}^2| - |k_F|^2 - \sqrt{(|\boldsymbol{k}|^2 - |k_F|^2)^2 + \tilde{\Delta}^2|k_F|^2|\boldsymbol{k}|^2}]/\tilde{\Delta}|\boldsymbol{k}|k_F e^{il\theta}$. We introduce an additional variational parameter, namely, a momentum cutoff $k_{\rm cutoff}$, analogous to the Debye cutoff of

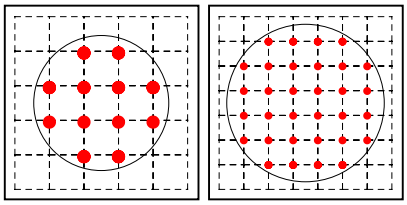

FIG. 1. Fermi seas for $N = 12$ and 32 composite fermions.

the BCS theory, by setting $g_{\boldsymbol{k}}^{(l)} = 0$ for $|\boldsymbol{k}| > k_{\rm cutoff}$. For $k_{\rm cutoff} = k_F$ the CF-BCS wave function reduces to the CFFS wave function [39,41,43]. The 221 state lies in the sector with Haldane pseudomomenta $(K_x, K_y) = (N/2, N/2)$, $(0, N/2)$ or $(N/2, 0)$ [44]; in what follows, we will choose our CF-BCS state in the sector $(K_x, K_y) = (N/2, N/2)$.

In the absence of LL mixing, the electron-electron interaction in the $n = 0$ LL of monolayer graphene is identical to that in the LLL of GaAs quantum well with zero width. The physics in the $n = 0$ LL of monolayer graphene is therefore identical to that in the LLL of GaAs quantum well (of zero width), including the state at half filling, which is well known to be a CFFS [45–47]. The interaction pseudopotentials in the $n \neq 0$ LLs of monolayer graphene are different from those in the corresponding LLs of semiconductor quantum wells. We numerically investigate the candidate states at half filling in the $|n| = 1$, $|n| = 2$, and $|n| = 3$ LLs of graphene.

The interelectron interaction in any given LL is completely specified by its Haldane pseudopotentials [6]. The problem of electrons in the nth LL can thus be mapped into the problem of electrons in the $n = 0$ LL with an effective interaction that has the same Haldane pseudopotentials as the Coulomb interaction in the nth LL. We consider two approximate real-space effective interactions [48,49]: $V_{\rm Toke} = r^{-1} + \sum_{i=0}^{6} c_i r^i e^{-r}$ and $V_{\rm Park}(r) = r^{-1} + a_1 e^{-\alpha_1 r^2} + a_2 r^2 e^{-\alpha_2 r^2}$. For the former, we obtain the coefficients by matching the first seven odd pseudopotentials of the effective interaction in LLL in the disk geometry with the pseudopotentials of the Coulomb interaction in the nth graphene LL [7,50–52]; for the latter, we match the first four odd pseudopotentials (in the $n = 2$ LL, we need to make an additional approximation, discussed in the Supplemental Material [23]). For the torus geometry, the interaction is replaced by an appropriate periodic interaction [23]. One expects that the nature of the state is dictated by the first few odd pseudopotentials (even pseudopotentials are not germane for fully spin-polarized electrons). To test the validity of the two effective interactions, we compare their energies with the exact Coulomb energies for certain CF-BCS wave functions for $N = 12$ particles in the $n = 2$ and $n = 3$ graphene LLs. We find that both effective interactions are satisfactory for the $n = 2$ LL, whereas only the Park interaction is satisfactory for the $n = 3$ LL. Below we assume spin-polarized electrons, disregard LL mixing, and quote all energies in units of $e^2/\epsilon\ell$.

We have calculated the energies of the CF-BCS wave function using the lattice Monte Carlo method [53], which allows us to go to fairly large systems. We have considered systems with 12 and 32 particles because the Fermi seas for these systems are close to being circular (Fig. 1). Figure 2 shows the minimum energy in $n = 2$ and $n = 3$ graphene LLs as a function of the gap parameter $\tilde{\Delta}$ where each point is obtained by minimizing the energy with respect to $k_{\rm cutoff}$. Because the CFFS is a special case of the BCS-p and the BCS-f states (obtained with $k_{\rm cutoff} = k_F$), the minimum energy is guaranteed to be less than or equal to that of the energy of the CFFS. Energy less than that of the CFFS implies a pairing instability of the CFFS.

As shown in Fig. 2, the lowest energy state in $n = 3$ graphene LL is obtained for the BCS-f state. Interestingly,

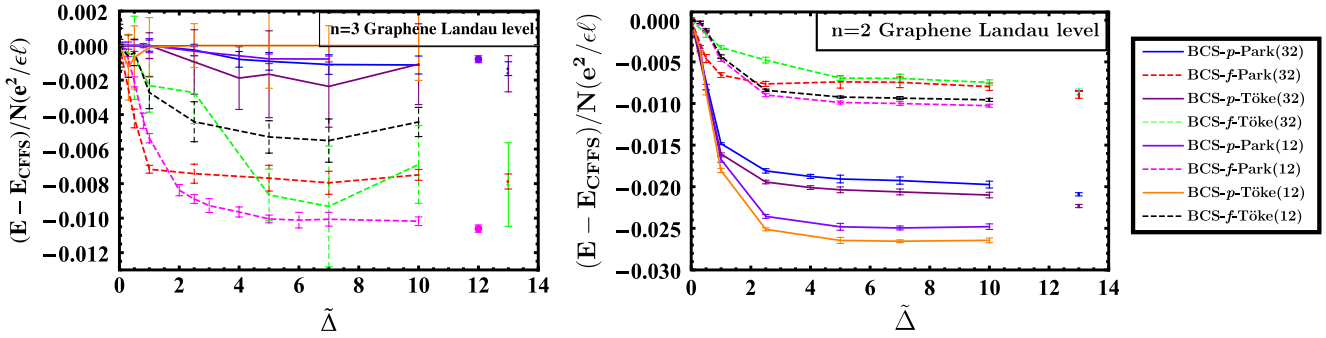

FIG. 2. Energy per particle of the BCS-p and BCS-f wave states for the "Park" and "Tőke" forms for the interaction (Refs. [48,49]) for the $n = 3$ graphene LL (left panel) and $n = 2$ graphene LL (middle panel) as a function of the gap parameter $\tilde{\Delta}$ for systems of 12 and 32 particles. The energies are quoted in units of $e^2/\epsilon\ell$, and measured relative to the energy of the CFFS. The energies for the $\tilde{\Delta} \to \infty$ limit are marked as isolated points at the right side of each plot. The legends are listed in the right panel, with the number of particles given in parentheses.

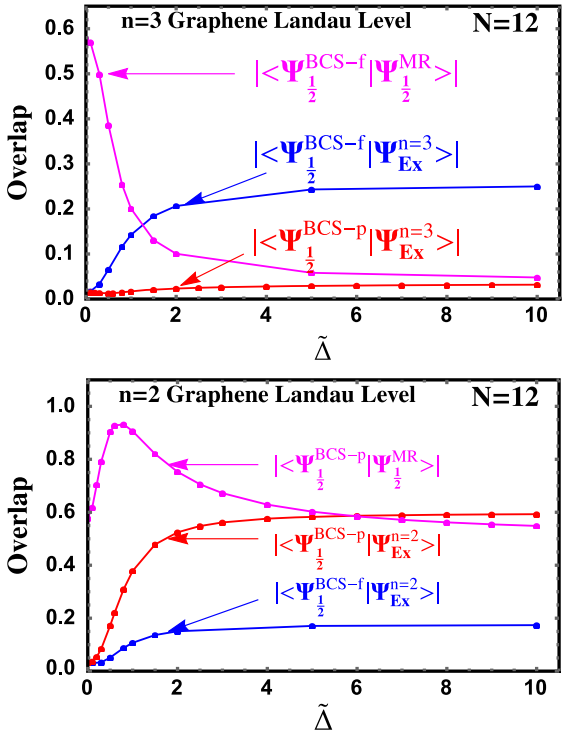

FIG. 3. Upper panel: Overlaps of the candidate states with the exact Coulomb ground state in the $n = 3$ graphene Landau level for 12 particles. The optimal overlap between the f-wave CF-BCS state and the exact ground state is approximately 0.25. The overlap of the p-wave paired state with the exact state is less than 0.025 for all values of $\tilde{\Delta}$. The overlap of the MR (p-wave) state with the exact Coulomb ground state in the $n = 3$ graphene LL is 0.01078. Lower panel: Overlaps of the candidate states with the exact Coulomb ground state in the $n = 2$ Landau level of graphene for 12 particles. The optimal overlap between the f-wave CF-BCS state and the exact ground state is approximately 0.174. The optimal overlap of the p-wave paired state with the exact state is 0.5928. The overlap of the MR (p-wave) state with the exact Coulomb ground state in the $n = 2$ LL of graphene is 0.19234.

the energy is insensitive to the variation of the gap parameter $\tilde{\Delta}$ for larger values. In fact, the optimal state is well approximated by the limit $\tilde{\Delta} \to \infty$, where the CF-BCS state simplifies with $g_k = -e^{-il\theta}$. The BCS-p state may have slightly lower energy than the CFFS, but has higher energy than the f-wave CF-BCS state.

Figure 3 shows the overlaps of the various candidate states with the exact ground state for the Coulomb interaction in graphene. For this purpose, we obtain the exact Fock-space representation of the CF-BCS state using the method in Ref. [54]. The overlap of the exact Coulomb ground state in graphene at the half-filled $n = 3$ LL with BCS-f state is approximately 0.25 in the parameter range where the energy is minimum. This overlap is not decisive, but still significant for an FQHE state in a high LL. (For the LLL, the wave functions of CFs at fractions $\nu = s/(2s \pm 1)$, s integer, have overlaps of ~0.99 with the Coulomb ground states for systems accessible to numerical diagonalization [5,55,56], but for the $n = 1$ LL in GaAs the overlaps are generally much smaller; for example, the $7/3$ and $5/2$ Coulomb ground states have overlaps in the ranges 0.5–0.7 and 0.7–0.9, respectively, with the Laughlin and MR wave functions for numerically accessible particle numbers [57–61]. We expect the overlaps to decrease further in yet higher LLs.) The BCS-f state is substantially better than other candidate states: the overlaps of the CFFS, BCS-p, and the MR-p states with the exact Coulomb ground state at half filling in the $n = 3$ graphene LL are, respectively, 0.015 44, ~0.025, and 0.010 78 (we have used the MR-p wave function given in Refs. [62–64]). The CF-BCS state is also better than the 12-particle 221 state, which has an overlap of 0.09 with the exact Coulomb ground state in the $n = 3$ graphene LL in the spherical geometry [7]. Our work thus provides important theoretical support to f-wave pairing in the half-filled $n = 3$ graphene LL. Given that our results for 12 and 32 particles are quite consistent, we speculate that for this problem, the torus geometry may better represent the thermodynamic behavior than the spherical geometry used in Ref. [7]. Exact diagonalization of the Coulomb interaction on torus with $\tau = i$ shows that the ground states for $N = 8$, 12, 14, and 16 particles lie in the sector with Haldane pseudomomenta $(K_x, K_y) = (N/2, N/2)$, $(0, N/2)$ or $(N/2, 0)$, which are the momentum sectors for the paired state [44]. As shown in the Supplemental Material, the BCS-f-wave state can be made more robust by modifying the interaction [23].

Figure 2 also shows the results for $N = 12$ and 32 particles at half filling in the $n = 2$ graphene LL. The lowest energy is obtained for the p-wave paired state. The overlap of the 12 particle CF-BCS state with the exact Coulomb state is ~0.6 (Fig. 3). Intuitively, a p-wave pairing would not be entirely surprising here, as the $n = 2$ graphene LL wave function is a combination of the $n = 2$ and $n = 1$ GaAs LL wave functions, the latter of which is believed to support p-wave pairing [50,58,59,61,65,66].

Our study does not decisively prove CF pairing in $n = 2$ and $n = 3$ graphene LLs, as we have not ruled out all possible states such as the stripe phase. Nevertheless, we conclude that a paired state is at least competitive, and that *if* FQHE is observed at half filling in the $n = 3$ ($n = 2$) graphene LL, it is likely an f-wave (a p-wave) paired state. It is noted that $1/2$ FQHE has not yet been observed in the $n = 2$ graphene LL [67,68]; we have not considered the possibility of whether the paired state can be destabilized by LL mixing.

We find no pairing instability at half filling in the $n = 1$ graphene LL, i.e., our calculations show that the lowest energy is obtained when $k_{\text{cutoff}} = k_F$ for arbitrary $\tilde{\Delta}$. This is in agreement with earlier variational and exact

diagonalization studies [56,69–72]. The observation of many fractions along the sequences $\nu = s/(2s \pm 1)$ [73] is consistent with a CFFS at $\nu = 1/2$.

The BCS-f state is topologically distinct from the BCS-p wave state. The thermal Hall conductance at temperature T, which is given by $\kappa = c(\pi^2 k_B^2/3h)T$ where c is the chiral central charge [74], can, in principle, distinguish between them [9,10,75]. The chiral central charge for different paired CF states is given by the relation $c = (1 + l/2)$; in particular, for the p and f states considered here it is given by $c = 3/2$ and $5/2$. The Hall viscosity η^A [76] is given by [77] $\eta^A = \hbar\rho\mathcal{S}/4$, where ρ is the 2D density and $\mathcal{S} = N/\nu - N_\phi$ is the "shift" [78] in the spherical geometry. For the p and f states at $\nu = 1/2$ we have $\mathcal{S} = 3$ and 5, respectively.

What is the mechanism of pairing? It is known empirically that a CFFS is obtained when the short distance repulsion between electrons is dominant, as is the case in the $n = 0$ LL. When the short distance repulsion is reduced, which is what happens in higher LLs, the effective interaction between CFs may become attractive, causing pairing. We do not have a simple way to predict which pairing is preferred without performing a detailed calculation. A Chern-Simons based analysis of gauge fluctuations, as in Ref. [79], could provide further insight into this question.

In summary, we have determined the optimal pairing at half filling in graphene LLs in a CF-BCS approach. We find an absence of pairing instability in the $n = 0$ and $n = 1$ LLs but CF pairing appears possible in $n = 2$ and $n = 3$ LLs. Our primary conclusion is that if FQHE is observed in the $n = 2$ ($n = 3$) graphene LL, it likely represents p (f) wave pairing of CFs. Further experimental investigations of these states will be necessary for a definitive confirmation of their physical origin.

A. S. and J. K. J. thank the U.S. National Science Foundation for financial support under Grant No. DMR-2037990. S. P. was supported (at Penn State) by the U.S. Department of Energy, Office of Basic Energy Sciences, under Grant No. DE-SC-0005042 and is supported (at Leeds) by the Leverhulme Trust Research Leadership Award RL-2019-015 and EPSRC Grant EP/R020612/1. A. C. B. acknowledges the Science and Engineering Research Board (SERB) of the Department of Science and Technology (DST) for financial support through the Start-up Grant SRG/2020/000154. We have made use of Advanced CyberInfrastructure computational resources provided by The Institute for CyberScience at The Pennsylvania State University. We thank M. Wimmer for the open-source PFAPACK library [80], used for the numerical evaluation of the Pfaffian of matrices. We are grateful to the authors of the DiagHam package, which we used for some of our exact diagonalization calculations.

[1] R. Willett, J. P. Eisenstein, H. L. Störmer, D. C. Tsui, A. C. Gossard, and J. H. English, Observation of an Even-Denominator Quantum Number in the Fractional Quantum Hall Effect, Phys. Rev. Lett. **59**, 1776 (1987).
[2] G. Moore and N. Read, Nonabelions in the fractional quantum Hall effect, Nucl. Phys. **B360**, 362 (1991).
[3] N. Read and D. Green, Paired states of fermions in two dimensions with breaking of parity and time-reversal symmetries and the fractional quantum Hall effect, Phys. Rev. B **61**, 10267 (2000).
[4] J. K. Jain, Composite-Fermion Approach for the Fractional Quantum Hall Effect, Phys. Rev. Lett. **63**, 199 (1989).
[5] J. K. Jain, *Composite Fermions* (Cambridge University Press, New York, US, 2007).
[6] F. D. M. Haldane, Fractional Quantization of the Hall Effect: A Hierarchy of Incompressible Quantum Fluid States, Phys. Rev. Lett. **51**, 605 (1983).
[7] Y. Kim, A. C. Balram, T. Taniguchi, K. Watanabe, J. K. Jain, and J. H. Smet, Even denominator fractional quantum Hall states in higher Landau levels of graphene, Nat. Phys. **15**, 154 (2019).
[8] J. K. Jain, Incompressible quantum Hall states, Phys. Rev. B **40**, 8079 (1989).
[9] A. C. Balram, M. Barkeshli, and M. S. Rudner, Parton construction of a wave function in the anti-Pfaffian phase, Phys. Rev. B **98**, 035127 (2018).
[10] W. N. Faugno, A. C. Balram, M. Barkeshli, and J. K. Jain, Prediction of a Non-Abelian Fractional Quantum Hall State with f-Wave Pairing of Composite Fermions in Wide Quantum Wells, Phys. Rev. Lett. **123**, 016802 (2019).
[11] X. G. Wen, Non-Abelian Statistics in the Fractional Quantum Hall States, Phys. Rev. Lett. **66**, 802 (1991).
[12] S. Bandyopadhyay, L. Chen, M. T. Ahari, G. Ortiz, Z. Nussinov, and A. Seidel, Entangled Pauli principles: The DNA of quantum Hall fluids, Phys. Rev. B **98**, 161118(R) (2018).
[13] Y. Wu, T. Shi, and J. K. Jain, Non-Abelian parton fractional quantum Hall effect in multilayer graphene, Nano Lett. **17**, 4643 (2017).
[14] S. A. Trugman and S. Kivelson, Exact results for the fractional quantum Hall effect with general interactions, Phys. Rev. B **31**, 5280 (1985).
[15] J. Shabani, T. Gokmen, and M. Shayegan, Correlated States of Electrons in Wide Quantum Wells at Low Fillings: The Role of Charge Distribution Symmetry, Phys. Rev. Lett. **103**, 046805 (2009).
[16] J. Shabani, T. Gokmen, Y. T. Chiu, and M. Shayegan, Evidence for Developing Fractional Quantum Hall States at Even Denominator 1/2 and 1/4 Fillings in Asymmetric Wide Quantum Wells, Phys. Rev. Lett. **103**, 256802 (2009).
[17] J. Shabani, Y. Liu, M. Shayegan, L. N. Pfeiffer, K. W. West, and K. W. Baldwin, Phase diagrams for the stability of the $\nu = \frac{1}{2}$ fractional quantum Hall effect in electron systems confined to symmetric, wide GaAs quantum wells, Phys. Rev. B **88**, 245413 (2013).
[18] G. Möller and S. H. Simon, Paired composite-fermion wave functions, Phys. Rev. B **77**, 075319 (2008).
[19] A. Sharma, S. Pu, and J. K. Jain, Bardeen-Cooper-Schrieffer pairing of composite fermions, Phys. Rev. B **104**, 205303 (2021).

[20] G. Wagner, D. X. Nguyen, S. H. Simon, and B. I. Halperin, *s*-Wave Paired Electron and Hole Composite Fermion Trial State for Quantum Hall Bilayers with $\nu = 1$, Phys. Rev. Lett. **127**, 246803 (2021).

[21] R. C. Gunning and A. Brumer, *Lectures on Modular Forms. (AM-48)* (Princeton University Press, Princeton, NJ, 1962).

[22] P. G. De Gennes, *Superconductivity of Metals and Alloys*, Advanced Book Classics (Perseus, Cambridge, MA, 1999).

[23] See Supplemental Material at http://link.aps.org/supplemental/10.1103/PhysRevLett.130.126201, which includes a brief review of the CF-BCS wave function, a discussion of the Haldane pseudopotentials and the effective interaction, technical details of the energy calculation, several consistency checks and includes Refs. [24–32].

[24] D. Yoshioka, B. I. Halperin, and P. A. Lee, Ground State of Two-Dimensional Electrons in Strong Magnetic Fields and $\frac{1}{3}$ Quantized Hall Effect, Phys. Rev. Lett. **50**, 1219 (1983).

[25] G. J. Sreejith, Y.-H. Wu, A. Wójs, and J. K. Jain, Tripartite composite fermion states, Phys. Rev. B **87**, 245125 (2013).

[26] M. Fremling, T. H. Hansson, and J. Suorsa, Hall viscosity of hierarchical quantum Hall states, Phys. Rev. B **89**, 125303 (2014).

[27] M. Greiter, V. Schnells, and R. Thomale, Laughlin states and their quasiparticle excitations on the torus, Phys. Rev. B **93**, 245156 (2016).

[28] K. K. W. Ma, Identification of topological order in the fractional quantum Hall state at $\nu = 1/4$, Phys. Rev. B **100**, 205306 (2019).

[29] S. Pu, M. Fremling, and J. K. Jain, Hall viscosity of composite fermions, Phys. Rev. Res. **2**, 013139 (2020).

[30] S. Pu and J. K. Jain, Composite anyons on a torus, Phys. Rev. B **104**, 115135 (2021).

[31] A. C. Balram, A non-Abelian parton state for the $\nu = 2 + 3/8$ fractional quantum Hall effect, SciPost Phys. **10**, 83 (2021).

[32] K. Bose and A. C. Balram, Prediction of non-Abelian fractional quantum Hall effect at $\nu = 2 + 4/11$ (2023), arXiv:2302.02478.

[33] J. K. Jain and R. K. Kamilla, Composite fermions in the Hilbert space of the lowest electronic Landau level, Int. J. Mod. Phys. B **11**, 2621 (1997).

[34] J. K. Jain and R. K. Kamilla, Quantitative study of large composite-fermion systems, Phys. Rev. B **55**, R4895 (1997).

[35] R. V. Mishmash, D. F. Mross, J. Alicea, and O. I. Motrunich, Numerical exploration of trial wave functions for the particle-hole-symmetric Pfaffian, Phys. Rev. B **98**, 081107(R) (2018).

[36] R. B. Laughlin, Anomalous Quantum Hall Effect: An Incompressible Quantum Fluid with Fractionally Charged Excitations, Phys. Rev. Lett. **50**, 1395 (1983).

[37] F. D. M. Haldane and E. H. Rezayi, Periodic Laughlin-Jastrow wave functions for the fractional quantized Hall effect, Phys. Rev. B **31**, 2529 (1985).

[38] F. D. M. Haldane, Many-Particle Translational Symmetries of Two-Dimensional Electrons at Rational Landau-Level Filling, Phys. Rev. Lett. **55**, 2095 (1985).

[39] S. Pu, Hall viscosity of the composite-fermion fermi seas for fermions and bosons, Phys. Rev. B **102**, 165101 (2020).

[40] S. Pu, Y.-H. Wu, and J. K. Jain, Composite fermions on a torus, Phys. Rev. B **96**, 195302 (2017).

[41] S. Pu, M. Fremling, and J. K. Jain, Berry phase of the composite-fermion Fermi sea: Effect of Landau-level mixing, Phys. Rev. B **98**, 075304 (2018).

[42] D. Mumford, *Tata Lectures on Theta Vols. I & II* (Birkhäuser, Boston, 2007).

[43] E. H. Rezayi and F. D. M. Haldane, Incompressible Paired Hall State, Stripe Order, and the Composite Fermion Liquid Phase in Half-Filled Landau Levels, Phys. Rev. Lett. **84**, 4685 (2000).

[44] A. Sharma, S. Pu, A. C. Balram, and J. K. Jain (unpublished).

[45] B. I. Halperin, P. A. Lee, and N. Read, Theory of the half-filled Landau level, Phys. Rev. B **47**, 7312 (1993).

[46] B. I. Halperin, the half-full Landau level, in *Fractional Quantum Hall Effects: New Developments*, edited by B. I. Halperin and J. K. Jain (World Scientific Pub Co Inc, Singapore, 2020), Chap. 2, pp. 79–132.

[47] M. Shayegan, Probing composite fermions near half-filled Landau levels, in *Fractional Quantum Hall Effects: New Developments*, edited by B. I. Halperin and J. K. Jain (World Scientific Pub Co Inc, Singapore, 2020), Chap. 3, pp. 133–181.

[48] K. Park, V. Melik-Alaverdian, N. E. Bonesteel, and J. K. Jain, Possibility of *p*-wave pairing of composite fermions at $\nu = 1/2$, Phys. Rev. B **58**, R10167 (1998).

[49] C. Töke, M. R. Peterson, G. S. Jeon, and J. K. Jain, Fractional quantum Hall effect in the second Landau level: The importance of inter-composite-fermion interaction, Phys. Rev. B **72**, 125315 (2005).

[50] K. Nomura and A. H. MacDonald, Quantum Hall Ferromagnetism in Graphene, Phys. Rev. Lett. **96**, 256602 (2006).

[51] C. Tőke, P. E. Lammert, V. H. Crespi, and J. K. Jain, Fractional quantum Hall effect in graphene, Phys. Rev. B **74**, 235417 (2006).

[52] C. Tőke and J. K. Jain, SU(4) composite fermions in graphene: Fractional quantum Hall states without analog in GaAs, Phys. Rev. B **75**, 245440 (2007).

[53] J. Wang, S. D. Geraedts, E. H. Rezayi, and F. D. M. Haldane, Lattice Monte Carlo for quantum Hall states on a torus, Phys. Rev. B **99**, 125123 (2019).

[54] G. J. Sreejith, A. Wójs, and J. K. Jain, Unpaired Composite Fermion, Topological Exciton, and Zero Mode, Phys. Rev. Lett. **107**, 136802 (2011).

[55] B. Yang and A. C. Balram, Elementary excitations in fractional quantum Hall effect from classical constraints, New J. Phys. **23**, 013001 (2021).

[56] A. C. Balram, Transitions from Abelian composite fermion to non-Abelian parton fractional quantum Hall states in the zeroth Landau level of bilayer graphene, Phys. Rev. B **105**, L121406 (2022).

[57] N. d'Ambrumenil and A. M. Reynolds, Fractional quantum Hall states in higher Landau levels, J. Phys. C **21**, 119 (1988).

[58] R. H. Morf, Transition from Quantum Hall to Compressible States in the Second Landau Level: New Light on the $\nu = 5/2$ Enigma, Phys. Rev. Lett. **80**, 1505 (1998).

[59] V. W. Scarola, J. K. Jain, and E. H. Rezayi, Possible Pairing-Induced Even-Denominator Fractional Quantum Hall Effect in the Lowest Landau Level, Phys. Rev. Lett. **88**, 216804 (2002).

[60] A. C. Balram, Y.-H. Wu, G. J. Sreejith, A. Wójs, and J. K. Jain, Role of Exciton Screening in the $\nu = 7/3$ Fractional Quantum Hall Effect, Phys. Rev. Lett. **110**, 186801 (2013).
[61] A. C. Balram and A. Wójs, Fractional quantum Hall effect at $\nu = 2 + 4/9$, Phys. Rev. Res. **2**, 032035(R) (2020).
[62] M. Greiter, X. Wen, and F. Wilczek, Paired Hall states, Nucl. Phys. **B374**, 567 (1992).
[63] S. B. Chung and M. Stone, Explicit monodromy of Moore–Read wavefunctions on a torus, J. Phys. A **40**, 4923 (2007).
[64] N. Read and E. Rezayi, Quasiholes and fermionic zero modes of paired fractional quantum Hall states: The mechanism for non-Abelian statistics, Phys. Rev. B **54**, 16864 (1996).
[65] M. O. Goerbig, R. Moessner, and B. Douçot, Electron interactions in graphene in a strong magnetic field, Phys. Rev. B **74**, 161407(R) (2006).
[66] M. O. Goerbig, Electronic properties of graphene in a strong magnetic field, Rev. Mod. Phys. **83**, 1193 (2011).
[67] G. Diankov, C.-T. Liang, F. Amet, P. Gallagher, M. Lee, A. J. Bestwick, K. Tharratt, W. Coniglio, J. Jaroszynski, K. Watanabe, T. Taniguchi, and D. Goldhaber-Gordon, Robust fractional quantum Hall effect in the $n = 2$ Landau level in bilayer graphene, Nat. Commun. **7**, 13908 (2016).
[68] S. Chen, R. Ribeiro-Palau, K. Yang, K. Watanabe, T. Taniguchi, J. Hone, M. O. Goerbig, and C. R. Dean, Competing Fractional Quantum Hall and Electron Solid Phases in Graphene, Phys. Rev. Lett. **122**, 026802 (2019).
[69] C. Tőke and J. K. Jain, Theoretical study of even denominator fractions in graphene: Fermi sea versus paired states of composite fermions, Phys. Rev. B **76**, 081403(R) (2007).
[70] A. Wójs, G. Möller, and N. R. Cooper, Composite fermion dynamics in half-filled Landau levels of graphene, Acta Phys. Pol. A **119**, 592 (2011).
[71] A. Wójs, G. Möller, and N. R. Cooper, Search for non-Abelian statistics in half-filled Landau levels of graphene, J. Phys. Conf. Ser. **334**, 012048 (2011).
[72] A. C. Balram, C. Tőke, A. Wójs, and J. K. Jain, Spontaneous polarization of composite fermions in the $n = 1$ Landau level of graphene, Phys. Rev. B **92**, 205120 (2015).
[73] F. Amet, A. J. Bestwick, J. R. Williams, L. Balicas, K. Watanabe, T. Taniguchi, and D. Goldhaber-Gordon, Composite fermions and broken symmetries in graphene, Nat. Commun. **6**, 5838 (2015).
[74] C. L. Kane and M. P. A. Fisher, Quantized thermal transport in the fractional quantum Hall effect, Phys. Rev. B **55**, 15832 (1997).
[75] E. Rowell, R. Stong, and Z. Wang, On classification of modular tensor categories, Commun. Math. Phys. **292**, 343 (2009).
[76] J. E. Avron, R. Seiler, and P. G. Zograf, Viscosity of Quantum Hall Fluids, Phys. Rev. Lett. **75**, 697 (1995).
[77] N. Read, Non-Abelian adiabatic statistics and Hall viscosity in quantum Hall states and $p_x + ip_y$ paired superfluids, Phys. Rev. B **79**, 045308 (2009).
[78] X. G. Wen and A. Zee, Shift and Spin Vector: New Topological Quantum Numbers for the Hall Fluids, Phys. Rev. Lett. **69**, 953 (1992).
[79] N. E. Bonesteel, I. A. McDonald, and C. Nayak, Gauge Fields and Pairing in Double-Layer Composite Fermion Metals, Phys. Rev. Lett. **77**, 3009 (1996).
[80] M. Wimmer, Algorithm 923: Efficient numerical computation of the Pfaffian for dense and banded skew-symmetric matrices, ACM Trans. Math. Softw. **38**, 1 (2012).